Fizika Nizkikh Temperatur, 2006, v. 32, Nos. 4/5, p. 602– 608

Correlated band structure of electron-doped cuprate materials

C. Dahnken[1], M. Potthoff[1], E. Arrigoni[2], and W. Hanke[1,3]

[1]*Institute for Theoretical Physics and Astrophysics, University of Würzburg, am Hubland, Würzburg 97074, Germany*
E-mail: arriqoni@itp.tu-graz.ac.at

[2]*Institute for Theoretical Physics and Computational Physics, Graz University of Technology, Graz, A-8010, Austria*

[3]*Kavli Institute for Theoretical Physics, University of California, Santa Barbara, California 93106-4030, USA*
E-mail: hanke@physik.uni-wuerzburg.de

Received August 25, 2005

We present a numerical study of the doping dependence of the spectral function of the *n*-type cuprates. Using a variational cluster-perturbation theory approach based upon the self-energy-functional theory, the spectral function of the electron-doped two-dimensional Hubbard model is calculated. The model includes the next-nearest neighbor electronic hopping amplitude t' and a fixed on-site interaction $U = 8t$ at half-filling and doping levels ranging from $x = 0.077$ to $x = 0.20$. Our results support the fact that a comprehensive description of the single-particle spectrum of electron-doped cuprates requires a proper treatment of strong electronic correlations. In contrast to previous weak-coupling approaches, we obtain a consistent description of the ARPES experiments *without* the need to (artificially) introduce a doping-dependent on-site interaction U.

PACS: 74.25.Jb, **74.72.—h**

Keywords: High-T_c superconductivity, cuprate materials, electron correlations.

Introduction

Angular resolved photoemission spectroscopy (ARPES) has greatly contributed to our current understanding of materials with strong electron correlations, in particular high-temperature superconductors (HTSC). Up to a few years ago, ARPES investigations have been concentrated on hole-doped HTSC materials. Since ARPES probes the part of the spectral function that is occupied by electrons, only the region below the insulating gap can be investigated in hole-doped cuprates. Although the observation of the unoccupied parts of the spectral function is in principle possible via inverse photoemission, the process is highly involved and does not yield the same resolution as direct photoemission. An opportunity for a more comprehensive study of the doping dependence of the spectral function is offered by electron-doped cuprates. In these materials, not only the excitations below the Fermi level in the *lower* Hubbard band, but also those below the Fermi level in the *upper* Hubbard band can be studied and thus a large part of the important low-energy excitations is covered. For this reason, the investigation of such *n*-type cuprates by ARPES provides a large amount of new information on the quasiparticle dynamics of HTSC cuprates.

Recently, an ARPES study of the doping dependence of the electron-doped cuprate $Nd_{2-x}Ce_xCuOCl_{4\pm\delta}$ (NCCO) has been carried out by the Stanford group [1,2]. In these measurements, the low-energy excitations of $Nd_2CuOCl_{4\pm\delta}$ (NCO) were shown to essentially coincide with the ones of typical undoped parent compounds of hole-doped materials such as $Sr_2CuO_2Cl_2$ and $Ca_2CuO_2Cl_2$, thus demonstrating the universality of the electronic structure of the (single layer) undoped cuprates. Upon electron doping, a remarkable Fermi surface (FS) evolution was found: In the heavily underdoped region the low-energy spectral weight is limited to an area close

around $\mathbf{k} = (\pi, 0)$. This has been interpreted as the formation of electron pockets. With increasing doping level, these pockets are connected by FS patches and finally form a large local density approximation (LDA)-like FS closed around $\mathbf{k} = (\pi, \pi)$.

The spectral function and FS data presented in [2] gave rise to several theoretical interpretations, which also include the idea of a collapse of the Mott gap due to strong suppression of the local Coulomb repulsion upon doping [3]. This conclusion was based upon mean-field calculations which employ a fitting of the on-site repulsion U_{eff} of the Hubbard model as a function of doping, to the value of the antiferromagnetic order parameter obtained from experiments at each doping level.

In the present paper, using both standard cluster-perturbation theory (CPT) [4–6] and, in particular, also a variationally improved version (V-CPT) [7–10], which is based on the self-energy functional theory [11], we calculate the spectral function of the two-dimensional one-band Hubbard model. This model is taken with next-nearest neighbor hopping amplitude $t' = -0.35t$ and fixed on-site interaction $U = 8t$ at half filling and doping levels ranging from $x = 0.077$ to $x = 0.20$. Our numerical results show that the salient features of the recent ARPES experiments for electron-doped cuprates can be reproduced with one-and-the-same Hubbard model without the necessity to resort to any change of the U-values as a function of doping as used in previous theoretical studies. Our challenge here is to reproduce the global (i.e. n- and p-doped) phase diagram by one universal choice of the model parameters, starting from a picture of a doped Mott–Hubbard insulator.

Model

As a generic model for the HTSC compounds we use the one-band Hubbard model [12] H_{1b}, i.e.

$$H_{1b} = -t \sum_{\langle i,j \rangle} (c^{\dagger}_{i\sigma} c_{j\sigma} + \text{h.c.}) + U \sum_{i} n_{i\uparrow} n_{i\downarrow}. \quad (1)$$

Here, $c^{\dagger}_{i\sigma}$ ($c_{i\sigma}$) creates (annihilates) an electron on site i with spin σ, $\langle \ldots \rangle$ denotes nearest neighbors and U is the on-site part of the Coulomb repulsion. Although the $t-U$ Hubbard model at low temperature develops a quasiparticle band of the appropriate width [13,14], the dispersion shows a near degeneracy between the $\mathbf{k} = (\pi, 0)$ and the $\mathbf{k} = (\pi/2, \pi/2)$ points. From ARPES experiments, however, we know that the quasiparticle peak at $\mathbf{k} = (\pi, 0)$ is shifted to higher binding energies. Actually, the dispersion of the quasiparticle peak shows two parabola with lowest binding energy at $\mathbf{k} = (\pi/2, 0)$ and $\mathbf{k} = (\pi, \pi/2)$. It is, thus, indispensable to add at least one additional term [15,16], which is taken here to be the hopping between next-nearest neighbors ($\langle\langle \ldots \rangle\rangle$), i.e.

$$-t' \sum_{\langle\langle i,j \rangle\rangle} (c^{\dagger}_{i\sigma} c_{j\sigma} + \text{h.c}). \quad (2)$$

Even longer-range hopping (t'') elements have been proposed to achieve consistency with experiment [17]. However, for the purpose of a qualitative analysis, it is sufficient to lift the degeneracy between $\mathbf{k} = (\pi, 0)$ and $\mathbf{k} = (\pi/2, \pi/2)$ and, thus, create the indirect gap as observed in experiments.

Numerical technique

Despite the considerable simplification arising from the use of an effective single-band model, the calculation of the spectral function of the Hubbard model still remains a difficult task. The calculation of this quantity by exact diagonalization is only possible for a small lattice of up to 4×4 sites, provided periodic boundary conditions are used. Larger lattice sizes can only be calculated by stochastic methods, such as the quantum Monte Carlo (QMC) technique [18] or the density matrix renormalization group algorithm (DMRG) [19]. While these techniques certainly represent powerful approaches to strongly-correlated electron systems, they are known to show disadvantages when applied to the present problem. In case of QMC, doping and low temperatures lead to the well-known sign problem, i.e. the computation time increases exponentially with T and system size [14,20]. DMRG, in contrast, is a ground state technique successfully applied for 1D and ladder systems, but displays convergence problems when applied to two-dimensional systems.

Recently, a strong-coupling perturbation theory has been developed for which the infinite lattice is subdivided into sufficiently small clusters that can be treated exactly, followed by an infinite-lattice expansion in powers of the hopping between the clusters [4–6]. The expansion in the intercluster hopping can be formally carried out up to arbitrary order following the diagrammatic method of Refs. 21–23. The lowest order of this strong-coupling expansion in the intercluster hopping has been termed «cluster perturbation theory» (CPT).

The CPT Green's function is given by

$$\mathbf{G}_{\infty} = \mathbf{G}_0 + \mathbf{G}_0\mathbf{T}\mathbf{G}_0 + \mathbf{G}_0\mathbf{T}\mathbf{G}_0\mathbf{T}\mathbf{G}_0 \ldots = [\mathbf{G}_0^{-1} - \mathbf{T}]^{-1}, \quad (3)$$

where $\mathbf{G}_{\infty}$ is the Green's function of the infinite system, $\mathbf{G}_0$ the cluster Green's function and $\mathbf{T}$ the inter-cluster hopping. All quantities are matrices with

indices referring to the particular cluster and to the sites within that cluster. CPT can be considered as a systematic approach with respect to the cluster size, i.e. it becomes exact in the limit $N_c \to \infty$, where N_c is the number of sites within a cluster. In addition, CPT provides approximate results for an infinitely large system: One of the advantages of this method is that the CPT Green's function is defined for any wave vector $\mathbf{k}$ in the Brillouin zone, contrary to common «direct» cluster methods, like QMC or exact diagonalization (ED), for which only a few momenta are available.

CPT results for static quantities as well as for the single-particle spectral function have been shown to agree very well with different exact analytical and numerical results [5,6]. On the other hand, there is also a serious disadvantage of CPT at this level: Namely, the method does not contain any self-consistent procedure which implies that symmetry-broken phases cannot be studied. We have recently proposed a variational approach (V-CPT) to this problem, which is based on the self-energy-functional approach (SFA). This method is explained in detail elsewhere [7,8,11]. We use V-CPT to calculate the Green's function of the half-filled Hubbard model with long-range antiferromagnetic order while plain CPT is used for the doped system. The extension to a doped system with *d*-wave superconductivity was presented in Refs. 10.

Results and discussion

We consider the above single-band Hubbard model with nearest- t and next-nearest-neighbor t' hopping at zero temperature. Useful parameterizations of the $t-t'-U$ Hubbard model can be taken from the literature [16,24]. We choose $t' = -0.35t$ and $U = 8t$ here, which yields a sufficiently accurate ratio for the Mott gap $\Delta \approx 4t$ and for the width of the quasiparticle band $W \approx 1t$, and fits the experimental dispersion of the quasiparticle band. For a reasonable approximation to the full many-body problem, CPT and V-CPT calculations for relatively large clusters are required. In this work, we have calculated the spectral function for half filling and for doped systems with $x = 0.07$ to 0.2. To achieve the smallest doping level, clusters consisting of 13 sites have been used.

Figure 1 displays the spectral function $A(\mathbf{k},\omega)$ of the half-filled ($x = 0.0$, panel A) and overdoped $t-t'-U$ Hubbard model ($x = 0.2$, panel B). The plots show $A(\mathbf{k},\omega)$ along the momenta $\Gamma = (0, 0) \to X = (\pi, 0) \to M = (\pi, \pi) \to \Gamma = (0, 0)$ through the Bril-

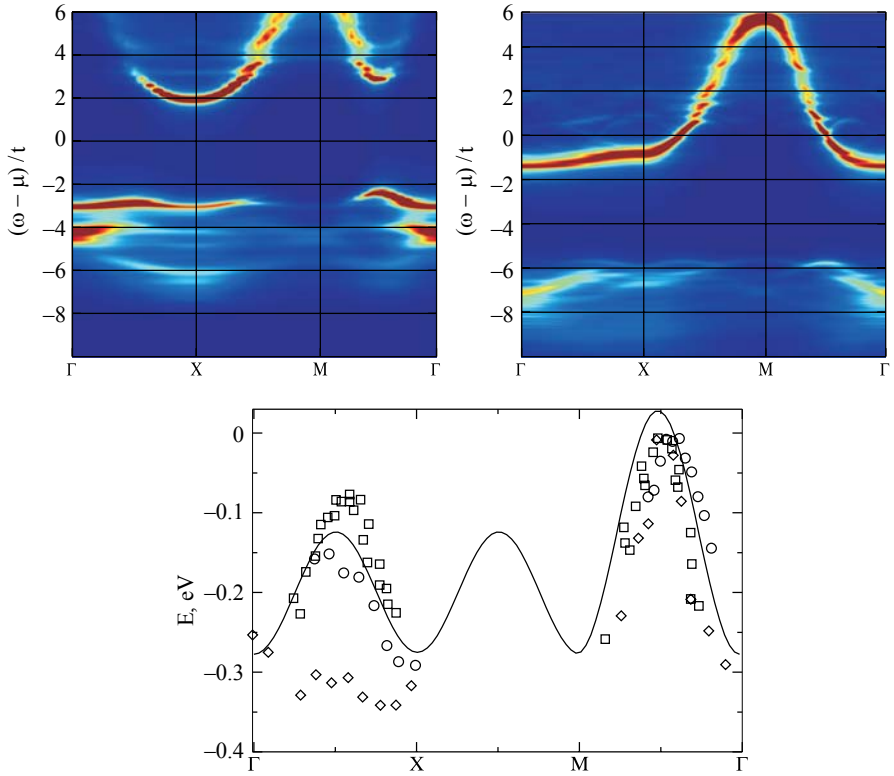

Fig. 1. Spectral function of the $t-t'-U$ Hubbard model with $t' = -0.35t$ and $U = 8t$. Panel A: half-filling. Panel B: overdoped system with $x = 0.2$. Panel C: Detailed dispersion of the quasiparticle band of panel A for $t = 0.5$ eV. Symbols represent the experimentally determined dispersion for $Sr_2CuO_2Cl_2$ (squares [25], circles [26], diamonds [27]). Both spectra where obtained by a CPT calculation using a 10-site cluster.

louin zone. The half-filled system in panel *A* gives rise to a narrow quasiparticle band, roughly between $\omega = -3t$ and $\omega = -2t$. A more detailed plot is given in panel *C*. One notices the characteristic parabolic dispersion close to $\mathbf{k} = (\pi/2, 0)$, $\mathbf{k} = (\pi, \pi/2)$ and $\mathbf{k} = (\pi/2, \pi/2)$. Assuming $t \approx 0.5$ eV, this dispersion is practically identical to the ARPES data [2,25,26,28]. The indirect single particle gap between $\mathbf{k} = (\pi, 0)$ and $\mathbf{k} = (\pi/2, \pi/2)$ is about $4t$, which is the maximum value still compatible with experiments.

At about $\omega = -3t$ a feature with maximal spectral weight close to $\mathbf{k} = (0, 0)$ can be observed. The same spectral feature was already observed in early QMC simulations of the single-band $t-U$ Hubbard model [29], exact diagonalizations of the $t-J$ model [30] and approximate perturbative methods such as the self-consistent Born approximation (SCBA). Its spectral weight was mostly perceived as coherent, i.e. corresponding to the «coherent» motion of a «spin-bag» like quasiparticle. This is also supported by more recent QMC simulations [13], V-CPT calculations [8] of the $t-U$ Hubbard model, and analytical considerations [31].

We now discuss the spectral function for the overdoped ($x = 0.2$) system, which is plotted in panel *B*. Here, one finds a metallic quasiparticle band with a flat dispersion just below the Fermi level at $\mathbf{k} = (\pi, 0)$. The band crosses the Fermi level close to $\mathbf{k} = (\pi/2, \pi/2)$ and $\mathbf{k} = (\pi, \pi/2)$ and therefore creates a large Fermi surface closed around $\mathbf{k} = (\pi, \pi)$ in the Brillouin zone. The quasiparticle band shows almost the same dispersion as the tight-binding ($U = 0$) model with the same parameterization. Deep below the Fermi level, between $\omega = -6t$ and $\omega = -10t$, we can see the traces of the lower Hubbard band observed at half filling, i.e. the area between $\omega = -4t$ and $\omega = -6t$ in panel *A*.

In Fig. 2 we plot a detail of the spectral function of the Hubbard model in a more restricted region around the Fermi level for three doping values, namely $x = 0.077$ (panel *A*), $x = 0.091$ (panel *B*), and $x = 0.200$ (panel *C*). For $x = 0.077$, the Fermi level enters into the upper Hubbard band with only slight modifications of the spectral weight. Most important, the arc around $\mathbf{k} = (\pi, 0)$ in the upper Hubbard band of the half-filled system is virtually unchanged and now forms an electron pocket around $\mathbf{k} = (\pi, 0)$, as can be seen in panel *A*. However, for this underdoped system, the Fermi level has not yet reached the bottom of the parabolic band around $\mathbf{k} = (\pi/2, \pi/2)$. The effect of doping is not limited to a rigid shift of the band structure with respect to the half-filled situation. As a matter of fact, some new spectral weight is created between $\omega = -1t$ and $\omega = -0.5t$ at $\mathbf{k} = (0, 0)$ and between $\omega = -0.5t$ and $\omega = 0t$ at $\mathbf{k} = (\pi/2, \pi/2)$. At higher doping, for $x = 0.091$ (panel *B*), this new spectral weight becomes more pronounced and starts producing the branches at $\mathbf{k} = (0, 0) \to (\pi, 0)$ and $\mathbf{k} = (0, 0) \to (\pi/2, \pi/2)$ below the Fermi level, which are clearly observed in the overdoped system in panel *C*.

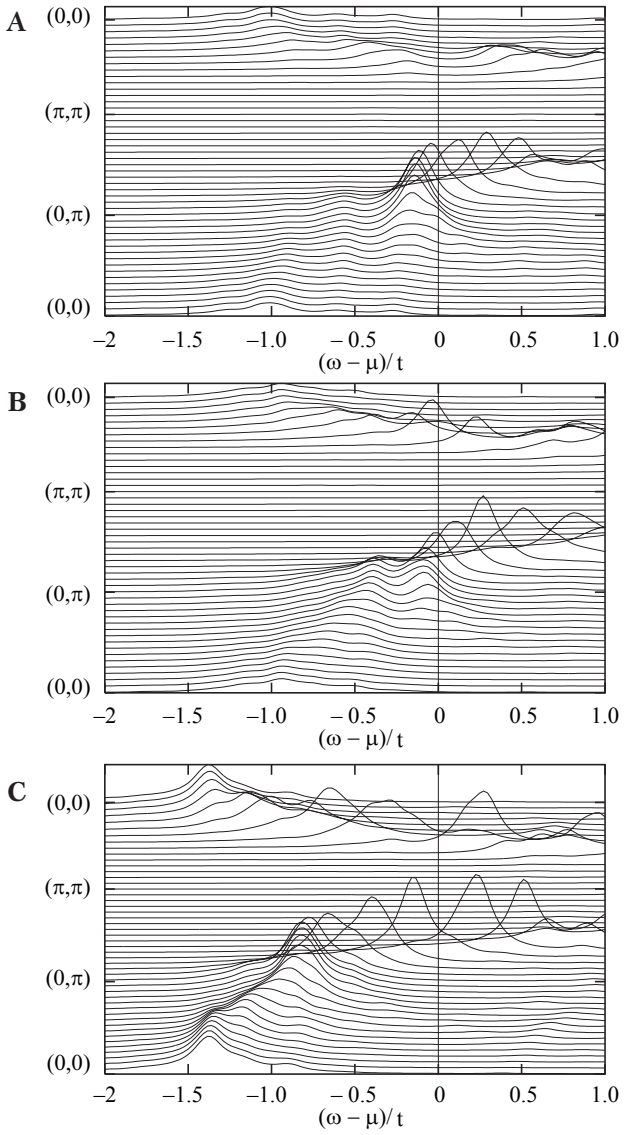

Fig. 2. Details of the spectral function of the $t-t'-U$ Hubbard model with $t' = -0.35t$ and $U = 8t$ restricted to a narrower region around the Fermi level. Panel *A*: $x = 0.077$, obtained from a 13 site cluster. Panel *B*: $x = 0.091$, obtained from a 11 site cluster. Panel *C*: $x = 0.200$, obtained from a 10 site cluster.

The results described above provide a deeper insight into the doping process of the $t-t'-U$ Hubbard model, provided one assumes that the parameters of the model do not change as a function of doping.

Although this assumption is widely believed to be appropriate for the doping range considered here, there have been suggestions that the on-site repulsion U is constant over a broader doping range. The possibility of a doping-dependent on-site repulsion was considered recently on the basis of a spin-density wave (SDW) mean field calculation of the $t - t' - t'' - U$ Hubbard model to describe the experimental data of the electron-doped system NCCO [2,3]. In contrast to the usual SDW calculation, where one self-consistently determines the single particle gap Δ_{mf} under the assumption that U is a fixed parameter, the authors of Ref. 3 consider U as a doping-dependent parameter fixed by the condition that at each doping value Δ_{mf} corresponds to the experimentally-determined pseudogap. In their calculation, which we herewith refer to as KMLB, the value of U_{eff} drops sharply upon doping from $U_{\text{eff}} = 6t$ at half filling to $U_{\text{eff}} \approx 3t$ at $x \approx 0.15$. The success of this idea is supported by the fact that the spectral function obtained from this procedure shows excellent agreement with the doping evolution of the experimentally observed Fermi surface. The whole scenario, however, is based upon the assumption that a varying U_{eff} is indispensable for the reproduction of the experimental results.

For this reason, it is important to verify, whether a doping-dependent U is necessary in order to correctly reproduce the spectral features as a function of doping, in particular the doping dependence of the Fermi surface. This is conveniently represented experimentally by plotting an intensity plot of the spectral weight at the Fermi energy $\omega = 0$. The upper row of Fig. 3 (panels A through C) shows the ARPES data taken from [2], whereas the lower row (panels D through F) plots the results obtained by in the CPT calculation [32].

Although we only used a minimal set of standard parameters and did not change the parameterization (in particular U) as a function of doping, the CPT Fermi surface of the fully correlated Hubbard model qualitatively reproduces the experimental result. In particular, we observe electron pockets around $\mathbf{k} = (\pi, 0)$ in the underdoped region, a FS patch at $\mathbf{k} = (\pi/2, \pi/2)$ for about $x = 0.10$ and a large FS centered around $\mathbf{k} = (\pi, \pi)$ in the overdoped case. All these features are consistent with the experimental results found in [2] as well as in the Hartree–Fock calculation of Ref. 3. As a matter of fact, Fig. 2 shows that the closing of the gap at higher doping, which is obtained «by hand» upon decreasing U within the KMLB, comes about naturally within our numerical treatment of the Hubbard model, in which electron correlations are treated more accurately.

Figure 4 directly compares the CPT and KMLB quasiparticle dispersion at half filling and $x = 0.10$ (CPT: $x = 0.091$). Notice that for the KMLB results only the dispersion is indicated (solid line). In order to have comparable energy scales, we reported the energies from [3] in unit of $t = 1$.

At half filling (Panel A) both methods show almost identical dispersions for the lowest-energy excitations, since both methods have been fitted to the experimental results. However, as a SDW-type mean field

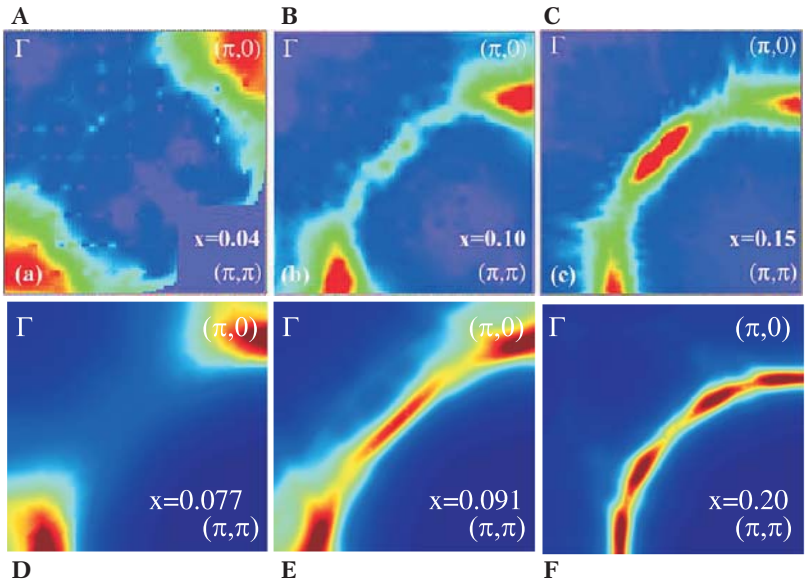

Fig. 3 Spectral weight at the Fermi energy, whose maximum is an indication of the Fermi-surface contour for different doping levels. The plots A through C are obtained from ARPES experiments (taken from [2]), while D through F correspond to our CPT results, whose spectral functions are plotted in Fig. 2.

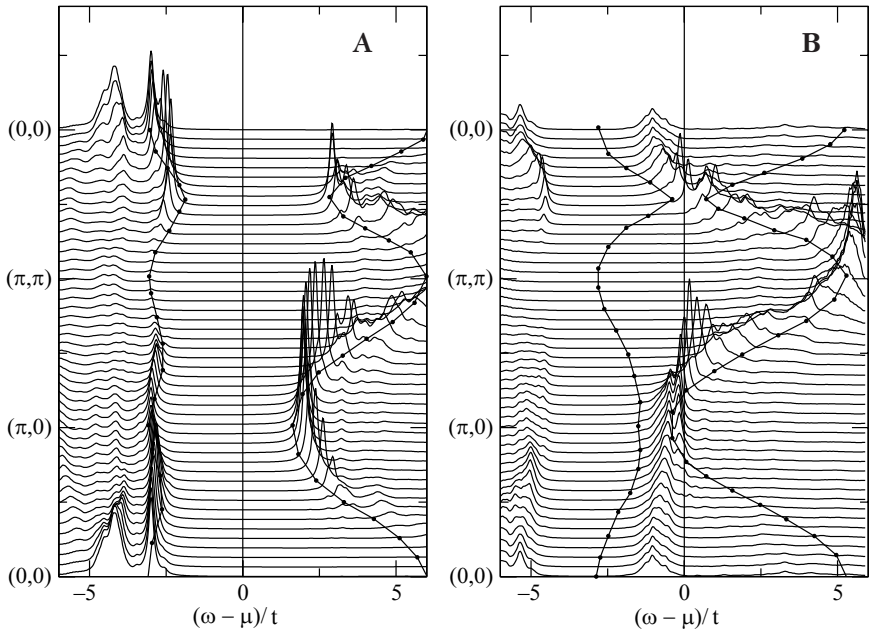

Fig. 4. Direct comparison between CPT and KMLB results (see text). The KMLB dispersion is indicated by the solid line. In both cases, energies are given in units of $t = 1$. *A*: half-filling; *B*: $x = 0.10$ (CPT $x = 0.091$).

method, the KMLB results cannot describe the full lower Hubbard band and is exclusively fitted to the low-energy excitations. Hence, the lower part of the spectrum between $\omega \approx -3t$ to $\omega \approx -4t$ cannot be reproduced within this technique.

Both techniques describe the closing of the gap as a function of doping. Although the CPT dispersion is much weaker and shows a much smaller gap at $\mathbf{k} = (\pi/2, \pi/2)$, the qualitative development as a function of doping is very similar. As discussed above, there is additional information provided by CPT in contrast to KMLB, concerning the high-binding energy part of the spectrum. In particular, a remainder of the parabolic dispersion at $\mathbf{k} = (\pi/2, \pi/2)$ is found at $\omega \approx -5t$. This feature does not appear in the mean field calculation, but can be clearly identified in the experimental data [2].

Conclusion

In conclusion, we have shown that the evolution of the Fermi surface of the electron-doped cuprates is well described within the framework of the one-band Hubbard model with nearest- and next-nearest-neighbor hoppings. In particular, we have provided indications that a doping-dependent Hubbard repulsion U is not necessary in order to describe the doping dependence of the ARPES spectrum.

The authors would like to acknowledge support by the DFG-Forschergruppe: Doping-dependence of phase transitions and ordering phenomena in cuprate superconductors (FOR 538), and by the Bavarian KONWHIR project CUHE. This research was supported in part by the National Science Foundation under Grant No. PHY99-0794. One of us (WH) would like to acknowledge the warm hospitality of the Kavli Institute for Theoretical Physics in Santa Barbara, where part of this work was concluded.

1. N.P. Armitage, D.H. Lu, C. Kim, A. Damascelli, K.M. Shen, F. Ronning, D.L. Feng, P. Bogdanov, Z.X. Shen, Y. Onose, Y. Taguchi, Y. Tokura, P.K. Mang, N. Kaneko, and M. Greven, *Phys. Rev. Lett.* **87**, 147003 (2001).
2. N.P. Armitage, F. Ronning, D.H. Lu, C. Kim, A. Damascelli, K.M. Shen, D.L. Feng, H. Eisaki, Z.-X. Shen, P.K. Mang, N. Kaneko, M. Greven, Y. Onose, Y. Taguchi, and Y. Tokura, *Phys. Rev. Lett.* **88**, 257001 (2002).
3. C. Kusko, R.S. Markiewicz, M. Lindroos, and A. Bansil, *Phys. Rev.* **B66**, 140513(R) (2002).
4. C. Gros and R. Valenti, *Phys. Rev.* **B48**, 418 (1993).
5. D. Sénéchal, D. Perez, and D. Plouffe, *Phys. Rev.* **B66**, 075129 (2002).
6. D. Sénéchal, D. Perez, and M. Pioro-Ladriere, *Phys. Rev. Lett.* **84**, 522 (2000).
7. M. Potthoff, M. Aichhorn, and C. Dahnken, *Phys. Rev. Lett.* **91**, 206402 (2003).
8. C. Dahnken, M. Aichhorn, W. Hanke, E. Arrigoni, and M. Potthoff, *Phys. Rev.* **B70**, 245110 (2004).
9. D. Sénéchal, P.L. Lavertu, M.A. Marois, and A.M.S. Tremblay, *Phys. Rev. Lett.* **94**, 156404 (2005).
10. M. Aichhorn and E. Arrigoni, *cond-mat/0502047 (unpublished).*

11. M. Potthoff, *Eur. Phys. J*. **B32**, 429 (2003).
12. J. Hubbard, *Proc. R. Soc. London* **276**, 238 (1963).
13. C.Göber, R. Eder, and W. Hanke, *Phys. Rev*. **B62**, 4336 (2000).
14. C. Gröber, *Ph. D. Thesis*, Universität Würzburg (1999).
15. T. Tohyama and S. Maekawa, *Supercond. Sci. Technol*. **13**, R17 (2000).
16. D. Duffy, A. Nazarenko, S. Haas, A. Moreo, J. Riera, and E. Dagotto, *cond-mat/9701083 (unpublished)*.
17. D. Senechal and A.-M. Tremblay, *Phys. Rev. Lett*. **92**, 126401 (2004).
18. J.E. Hirsch, *Phys. Rev*. **B38**, 12023 (1988).
19. R.M. Noack, S.R. White, and D.J. Scalapino, in: *Computer Simulations in Condensed Matter Physics VII*, D.P. Landau, K.K. Mon, and H.B. Schüttler (eds.), Spinger Verlag, Heidelberg, Berlin (1994).
20. H. Endres, *Ph. D. Thesis*, (1996).
21. W. Metzner, *Phys. Rev*. **B43**, 8549 (1991).
22. S. Pairault, D. Sénéchal, and A.M.S. Tremblay, *Eur. Phys. J*. **B16**, 85 (2000).
23. S. Pairault, D. Sénéchal, and A.-M.S. Tremblay, *Phys. Rev. Lett*. **80**, 5389 (1998).
24. W. Brenig, *Phys. Rep*. **251**, 154 (1995).
25. C. Dürr, S. Legner, R. Hayn, S.V. Borisenko, Z. Hu, A. Theresiak, M. Knupfer, M.S. Golden, J. Fink, F. Ronning, Z.-X. Shen, H. Eisaki, S. Uchida, C. Janowitz, R. Müller, R.L. Johnson, K. Rossnagel, L. Kipp, and G. Reichardt, *Phys. Rev*. **B63**, 014505 (2001).
26. S. LaRosa, I. Vobornik, F. Zwick, H. Berger, M. Grioni, G. Margaritondo, R.J. Kelley, M. Onellion, and A. Chubukov, *Phys. Rev*. **B56**, R525 (1997).
27. B.O. Wells, Z.-X. Shen, A. Matsuura, D.M. King, M.A. Kastner, M. Greven, and R.J. Birgeneau, *Phys. Rev. Lett*. **74**, 964 (1995).
28. F. Ronning, C. Kim, K. Shen, N. Armitage, A. Damascelli, D. Lu, D. Feng, Z.-X. Shen, L. Miller, Y.-J. Kim, F. Chou, and I. Terasaki, *cond-mat/0209651 (unpublished)*.
29. R. Preuss, W. Hanke, and W. von der Linden, *Phys. Rev. Lett*. **75**, 1344 (1995).
30. R. Eder and Y. Ohta, *Phys. Rev*. **B56**, 2542 (1997).
31. A. Dorneich, M.G. Zacher, C. Gröber, and R. Eder, *cond-mat/9909352 (unpublished)*.
32. Note that the doping levels are slightly different, since the available fillings in CPT are constrained by the cluster sizes.
33. Q. Yuan, F. Yuan, and C.S. Ting, *cond-mat/0503056 (unpublished)*.